Available online at www.sciencedirect.com
SCIENCE DIRECT®
Polymer 44 (2003) 4085–4096
polymer
www.elsevier.com/locate/polymer

Solid-state polymerization of PET: influence of nitrogen sweep and high vacuum

Y. Ma, U.S. Agarwal*, D.J. Sikkema, P.J. Lemstra

Polymer Technology Group, Faculty of Chemical Engineering, Dutch Polymer institute, Eindhoven University of Technology, Den Dolech 2, 5600 MB Eindhoven, The Netherlands

Received 20 February 2003; received in revised form 17 May 2003; accepted 20 May 2003

Abstract

We have examined the influence of reaction environment on the solid-state polymerization (SSP) of thin (180 μm) poly(ethylene terephthalate) (PET) chips at 250 °C by following the intrinsic viscosity (IV) increase and the end-group depletion. When the SSP reaction is carried out in vacuum, IV increases from 0.58 to 2.4 dl/g in 2.5 h of reaction. The initially rapid reaction slows considerably with time, and IV rise nearly stops at 2.75 dl/g at 6 h, though we still detect the acid and the hydroxyl end-groups at concentrations of 3 and 5 mequiv./kg, respectively. This suggests a role of crystallization in limiting the approachability of the end-groups to each other, thereby temporarily rendering them inactive. At this stage, raising the temperature to 270 °C to melt the PET in vacuum again increases the IV to 2.97 dl/g in 1.5 h, perhaps due to the release of crystalline restraints in the melt allowing some these inactive end-groups to approach each other. We find that accounting for these temporarily inactive end-groups is a must for a good kinetic description of SSP to IV $>$ 1.3 dl/g. When nitrogen is used as a carrier gas, the reaction rate and the extent of molecular weight build-up are somewhat lower compared to SSP under vacuum. A sublimate is collected during SSP under vacuum, and we find it to be made up of terephthalic acid, monohydroxyethyl terephthalate, bishydroxyethyl terephthalate and cyclic oligomers. This indicates the presence of a new condensation mechanism during SSP under vacuum.

Keywords: Poly(ethylene terephthalate); Solid-state polymerization; Kinetics

1. Introduction

Post polymerization of poly(ethylene terephthalate) (PET) in the solid-state is often utilized to enhance its number average molecular weight (M_n) beyond 20,000, desired for applications such as soft drink bottles, tire cord filaments and industrial fibers. The following reactions are generally considered to take place [1–5] when the solid PET pellets are heated to $T = 200–250$ °C

Transesterification/polycondensation

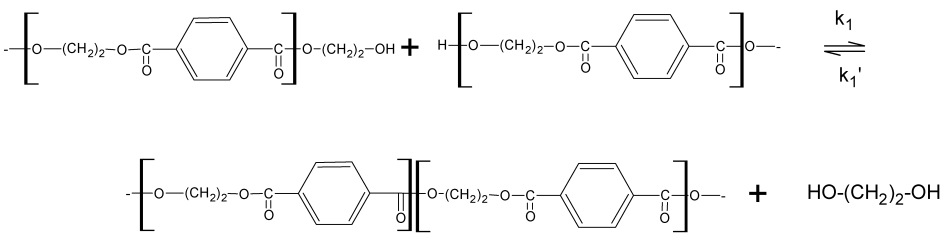

(1)

* Corresponding author. Tel.: +31-40-247-3079; fax: +31-40-243-6999.
E-mail address: u.s.agarwal@tue.nl (U.S. Agarwal).

0032-3861/03/$ - see front matter © 2003 Elsevier Science Ltd. All rights reserved.
doi:10.1016/S0032-3861(03)00408-7

Esterification

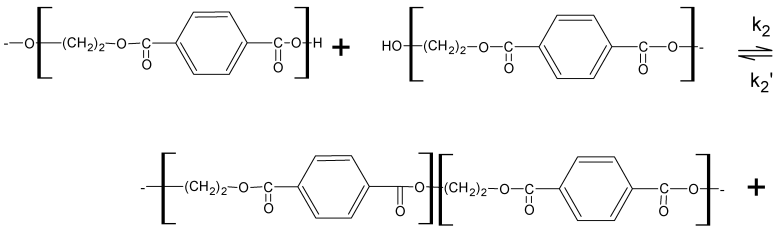

(2)

Here, water and ethylene glycol (EG) are the byproducts of the reversible reactions. The forward reactions are facilitated by the byproduct removal either by flow of inert gas or by maintaining reduced pressure, or a combination of the two [6,7]. The overall reaction rate is influenced by a combination of the intrinsic reaction rate [3,8–16], diffusion of the reactive end-groups [8,13,17–22] as limited by crystallization [23–25] or facilitated by interchange reactions [20], the diffusion of the byproducts from the pellet interior to the pellet surface [3,11,14,15,22,26] and their removal by the inert gas stream [8,13–15,22]. With the objective of obtaining high reaction rate, yet controlling the product quality as defined by the concentrations of the acid (COOH) and hydrodroxyl (OH) end-groups, diethylene glycol groups, and aldehydes, studies have been conducted to examine the influence of reaction parameters such as temperature [1,3,8–10,15,27–29], pellet size [3,8,9,23,27,28], crystallinity level [13,16,25,27,28], nature and rate of carrier gas [1,8,13,14,15,22], catalyst concentration [30,31], etc. In the absence of condensate diffusional limitations resulting in their fast removal, backward reactions are eliminated, and the reaction kinetics is described by the following expressions [4,13,14,21]

$$\frac{\mathrm{d[OH]}}{\mathrm{d}t} = -2R_{\mathrm{EG}} - R_{\mathrm{H_2O}} \tag{3}$$

$$\frac{\mathrm{d[COOH]}}{\mathrm{d}t} = -R_{\mathrm{H_2O}} \tag{4}$$

$$M_{\mathrm{n}} = \frac{2}{\mathrm{[OH]} + \mathrm{[COOH]}} \tag{5}$$

where

$$R_{\mathrm{EG}} = 2k_1[\mathrm{OH}]^2 \tag{6}$$

and

$$R_{\mathrm{H_2O}} = k_2[\mathrm{COOH}][\mathrm{OH}] \tag{7}$$

are the rates of production (or rates of removal) of EG and water, respectively. In Eq. (6), the additional factor of 2 is taken in to account for the two pairs of reaction sites for a given pair of chain-ends [32], the rate constants being taken as those corresponding to the reactive groups.

1.1. Ultrahigh molecular weight PET by SSP

While PET of intrinsic viscosity (IV) = 0.6–1.0 dl/g is useful for applications such as fibers, films and molding, its solid-state polymerization (SSP) to IV as high as 3 dl/g is desired for its solution spinning leading to high modulus high strength fibers [33–35]. The Table 1 summarizes the reports describing SSP of PET to IV higher than 1.5 dl/g or M_{n} higher than 70,000.

Of the above, only Hsu [8], Ito et al. [40] and Boiko and Marikhin [24] have reported kinetics data, though limited to IV(t) profiles. Further, the SSP summarized in Table 1 were conducted either only at atmospheric pressure (with nitrogen sweep) or only in vacuum. Thus, SSP under otherwise identical conditions, but differing in vacuum or carrier gas atmosphere, were not compared.

1.2. Depletion of end-groups during SSP

Several authors have followed the reduction in the OH and the COOH end-group concentrations with progress of SSP to moderate molecular weights, and their results are summarized in Table 2. These studies are all limited to M_{n} not exceeding 52,000, and it is only recently that Zhi-Lian et al. [14], Wu et al. [23] and Kang [21] have analyzed such end-group data in terms of the two simultaneous reactions (Eqs. (1) and (2)). Even these workers did not consider the role of crystallization in limiting the accessibility of the end-groups to each other. However, they did not face a contradiction in fitting the kinetics, because they limited their analysis to molecular weights less than 52,000. Duh [16] accounted for this role of crystallization, but ignored the esterification reaction (Eq. (2)), did not directly measure concentrations of the end-groups, and limited his analysis to IV less than 1.3 dl/g. Jabarin [43] and Wu et al. [23] reported that maximum SSP rate in palletized PET is achieved when [COOH]:[OH] = 0.5. Schaaf et al. [44] suggested an optimum at [COOH]:[OH] = 0.3 to 0.6 for maximum SSP rate. Chen and Chen [3] indicated that a high OH concentration is preferred in fine samples, while high COOH is preferred in granulated PET. However, during SSP of PET of IV = 0.25 dl/g, Duh [4] recently found monotonically decreasing SSP rates with increasing acid end-groups in starting PET.

The depletion of acid end-groups is generally attributed to the esterification reaction (Eq. (2)). Though it is generally believed that cyclic oligomers are removed by vacuum or inert gas [28], an alternative possibility is the sublimation of acid end-groups containing species such as terephthalic acid

Table 1
SSP of PET to ultrahigh molecular weight

Sl No.	Authors	Characteristics of initial PET	SSP conditions	Final M_n or IV (dl/g)
1	Hsu [8]	0.18–0.25 mm particle $M_n = 16,500$	250 °C, 40 h, $N_2 \sim 2$ cm/s	$M_n = 120,000$, IV = 2.27
2	Kurita et al. [36]	Standard chips, IV = 0.6	237 °C, 12 h, N_2	IV = 3.42
3	Cohn [37,38]	Porous fibrous pellet, IV = 1.9, $M_w = 100,800$	220–240 °C, 10 h, N_2	$M_n = 191,000$ IV = 5.3
4	Rinehart [39]	Porous pills made by compacting 0.84 mm particles, IV = 0.5	250 °C, 5 h, N_2	IV = 2.39
5	Ito et al. [33]	Solution grown crystals, 2–10μm, IV = 0.67	253 °C, 24 h, vacuum	IV = 2.41
6	Ito et al. [40,41]	Porous and fibrous aggregates IV = 0.61	240 °C, 12 h, 10 mtorr	IV = 3.2, up to 4.9 in multiple steps
7	Sasaki et al. [42]	Film, 0.01 mm, IV = 0.15	320 °C (melt), 1.5 min, 0.5 torr	IV = 2.31
8	Boiko and Marikhin [24]	100 μm film, $M_n = 15,000$	250 °C, 20 h, 0.05 mtorr	$M_n = 151,680$

(TA) and monohydroxyethyl terephthalate (MHET) at the high SSP temperatures under vacuum. An analysis of the sublimate during SSP will allow us to determine if such sublimation has a significant role to play.

1.3. Effect of nature and flow rate of carrier gas

Several authors have reported [1,8,14,15,26] that with increasing rate of carrier gas flow, the rate and the extent of post-polymerization increases, before leveling out at high flow rates. However, only Hsu [8] and Huang and Walsh [15] provided information on the gas velocity (perhaps the most direct parameter responsible for the mass transfer coefficient on the gas side) employed by them. Huang and Walsh [15] concluded that while nitrogen flow at 0.8 cm/s was sufficient to achieve maximum SSP rate in 1.1–2.7 mm particles at 190 °C, nitrogen flow at 2.5 cm/s was required to achieve the maximum reaction rate at 220 °C. Hsu [8] found that for SSP of 0.18–0.25 mm particles ($M_n = 16,500$) at 250 °C for 7 h, nitrogen flow at 2 cm/s lead to M_n of 58,000. However, use of helium or carbon dioxide under same conditions lead to M_n of 81,000 and 90,000, respectively. Hsu attributed this to the influence of carrier gas diffusion on the diffusivity of EG in the polymer, and to the interaction of the carrier gas with EG. Devotta and Mashelkar [13] quantified these effects in terms of the influence of the associated free volume changes on the diffusivities. Mallon et al. [45] found no discernible effect of carrier gases during SSP of 0.1 mm PET particles at 226 °C. Though Aharoni [6] indicated that nitrogen under reduced pressure performs better than either nitrogen sweep or high vacuum alone, Fakirov [8] suggested no significant influence of reaction medium (vacuum vs. nitrogen sweep) during SSP. A detailed analysis of such effects, if any, is not available. Chang et al. [28] found that vacuum (as compared to nitrogen sweep) gave better IV retention and less acid end-group production during annealing of PET (20–30 mesh, IV = 0.72 dl/g) for 2 h at 181 °C.

In this paper, we compare the kinetics of SSP to ultrahigh molecular weight under vacuum and under N_2 sweep. Not only the IV, but also the acid and hydroxyl end-groups concentrations are monitored using our recently developed NMR based technique [46]. The results are analyzed in terms of the kinetics of the two simultaneous reactions producing EG and water (Eqs. (1) and (2)), and additionally proposed reactions producing higher molar mass aromatic condensates. This possibility is examined by collection and analysis of the sublimate during the SSP process.

2. Experimental

2.1. Materials

PET chips were obtained from Wilton Research Center (ICI, UK), and the following characteristics were determined at Twaron Research (Arnhem): $M_n = 20,500$, DEG = 0.69 wt%, Sb = 212 ppm, Ti = 14 ppm, P = 78 ppm.

Chloroform ($CHCl_3$, 99.9%), deuterated chloroform ($CDCl_3$, 99.9 atom D%), phenol, tetrachloroethane (TCE, 97%), dimethyl sulfoxide (DMSO, d6, 99 atom D%), hexafluoroisopropanol (HFIP, 99%), α,α,α trifluorotoluene (TFT, 99%), 4-pyrrolidinopyridine (98%), trifluoroacetic acid (TFA, 99%) and bishydroxyethyl terephthalate (BHET) were obtained from Aldrich. Phenol (99%), NaOH (98%), EG (98%), dicyclohexyl carbodiimide (DCC, 99%), and TA (99%) were obtained from Merck. All chemicals were used as received.

2.2. NMR analysis

Varion Mercury Vx 400 was used to carry out the ^1H NMR and ^{19}F NMR measurements, using DMSO, $CDCl_3$, or $CDCl_3$ mixture with HFIP or TFA as the solvents.

2.3. Intrinsic viscosity of PET

The relative viscosity (η_{rel}) of solution of PET in phenol-TCE mixture (1:1, by weight) at concentration ($c = 0.5 \times$ g/dl) was determined using ubbelohde viscometer at 30 °C. IV was estimated from this single point measurement of η_{rel} and using the following approximation for linear flexible

Table 2
End-group depletion during SSP of PET

Sl No.	Authors	Characteristics of initial PET	SSP conditions	Initial and final M_n or IV (dl/g)	Initial and final [OH] (mequiv./kg)	Initial and final [COOH] (mequiv./kg)
1	Chen and Chen [3]	16–18 mesh particles	240 °C, 6 h, 60 mtorr	21,000, 52,000	56, 21	38, 16
2	Karayannidis et al. [29]	Precipitated PET	230 °C, 8 h, 30 mtorr	0.7, 1.5	56, 24	43, 08
3	Zhi-Lian et al. [14]	1.5 mm thick	225 °C, 30 h, N_2	22,000, 32,400	Not measured	20, 11.5
4	Wu et al. [23]	0.25 mm particles	235 °C, 4 h, 1 torr	18,000, 36,000	Not measured	30, 3

chains [47]:

$$\mathrm{IV} = (1/c)[2(\eta_{\mathrm{rel}} - 1) - 2\ln(\eta_{\mathrm{rel}})]^{1/2} \quad (8)$$

IV can be related to M_n using the Mark-Houwink relationship:

$$\mathrm{IV} = KM_n^a \quad (9)$$

Several workers have reported the coefficients K and a for measurements in the same mixed solvents, and these are summarized in Table 3.

2.4. Liquid chromatography–mass spectrometry (LC–MS)

The LC–MS system was Agilent (1100 series, MS type 61946D), using the column Supersphere RP18e, 150 × 3 mm, particle diameter 4 μm. The sample was dissolved in a mixture of HFIP/THF(1:10), and the following elution (0.4 ml/min) profile was used: MeOH/H_2O/THF = 50/50/0 for 10 min, then MeOH/H_2O/THF = 100/0/0 for 5 min, then wash out with THF. An electrospray interface was used to ionize the molecules. The drying gas temperature was 350 °C and flow rate was 10 l/min. The applied voltage on the capillary was 4 kV. The nebuliser pressure was 50 psi. Data was acquired in positive mode.

2.5. Solid-state polymerization in N_2 (SSP-N_2)

PET chips (average weight 0.045 g) were pressed for 1 min into thin disks (diameter ~1.5 cm, thickness ~180 μm) between two stainless steel plates heated to 160 °C, and these thin chips were used in all SSP experiments reported in this paper. These PET chips were suspended in a cylindrical (id = 27 mm) glass reactor immersed into preheated salt-bath, whose temperature was feedback controlled with a thermocouple placed in the reactor. Nitrogen gas flowing at the rate of 1 l/min (room temperature and pressure) was dried by passing through an anhydrous $CaSO_4$ column (W.H. Hammod Drierite, Xenia, Ohio), preheated by passing through a glass coil immersed in the same bath, and introduced at the bottom of the reactor. The nitrogen gas passed around the thin chips at a superficial velocity of 5 cm/s. Effectively higher velocities of 17 and 59 cm/s were achieved by keeping the nitrogen volumetric flow rate unchanged, but restricting the nitrogen flow through smaller cross-sections (id = 15, 8 mm) of the reactor. The chips were first dried in a reactor at 165 °C for 6 h. The chips were then transferred to another identical reactor, but maintained at 250 °C, and withdrawn after the desired time of reaction.

2.6. Sublimate collection during SSP-N_2

The SSP was conducted as above for 6 h at 250 °C using thin PET chips (1 g), the outgoing gases were passed through a cold trap (glass coil, immersed in liquid nitrogen, path length = 0.3 m, id = 7 mm), and then bubbled through $CHCl_3$ before being let out to the exhaust. No sublimate was observed on the reactor walls, the transfer lines, and in the cold trap. The $CHCl_3$ in the bath could be evaporated without leaving any residue.

2.7. Solid-state polymerization in vacuum (SSP-vacuum)

Thin PET chips were placed in a glass made 150 ml round bottomed flask connected to a vacuum pump maintaining 10 mtorr pressure. The flask was immersed till its neck into a preheated, temperature controlled salt bath. The chips were first dried at 165 °C for 6 h. The flask was then transferred to an identical bath but maintained at 252 °C (resulting in 250 °C inside the flask), and the flask was withdrawn after the desired time of reaction.

2.8. Sublimate collection during SSP-vacuum

The SSP was conducted with thin PET chips (1 g) as above for 3 h at 250 °C. The sublimate accumulated as a white film like deposit on the cooler sections of the flask (i.e. on walls at the mouth of the flask just outside of the salt-bath), and was collected by scrapping with a spatula.

Table 3
Coefficients of Mark-Houwink relationships (Eq. (9)) for PET in phenol:TCE (1:1 by wt)

Author	T (°C)	$K \times 10^4$	a	M_n range $\times 10^{-3}$
Koepp and Werner [48]	20	7.55	0.685	3–30
Conix [49]	25	2.1	0.82	5–25
Griehl and Neue [50]	20	1.27	0.86	5–21 (non-fractionated)
Griehl and Neue [50]	20	0.9	0.87	5–21 (fractionated)

2.9. Determination of acid end-groups in PET

The fluoroderivatization of the acid end-groups was carried out by DCC mediated esterification with HFIP [46]:

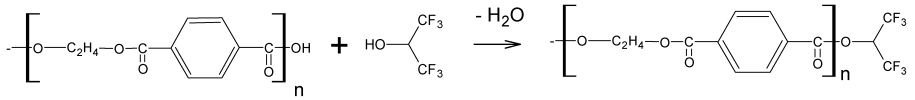

One chip of PET (0.045 g) was dissolved in a mixture of HFIP (0.2 g) and $CDCl_3$ (1.00 g) at room temperature. Firstly, part (0.1 g) of a solution of 4-pyrrolidinopyridine (0.001 g) in $CDCl_3$ (1 g) was added and subsequently, part (0.2 g) of a solution of DCC (0.0075 g) in $CDCl_3$ (1.5 g) was added. Finally, part (0.1 g) of a solution of TFT (0.01 g) in $CDCl_3$ (2 g) was added to the above reaction mixture to give the sample for ^{19}F NMR analysis. Integration of the $\delta -73.41$ [d, 6F] peak for the fluoroester relative to the $\delta -62.9$ [s, 3F] peak of TFT allowed quantification of the acid end-groups.

2.10. Determination of hydroxyl end-groups in PET

The hydroxyl end-groups were fluoroderivatized by esterification with TFA [46,51]:

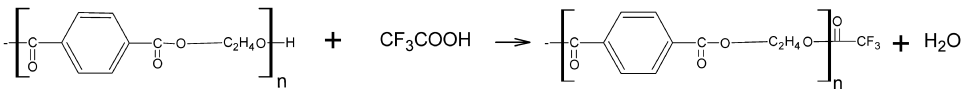

(11)

One chip of PET (0.045 g) was dissolved in a mixture of TFA (0.2 g) and $CDCl_3$ (1.0 g). Part (0.1 g) of a solution of TFT (0.01 g) in $CDCl_3$ (2 g) was added to the above reaction mixture. ^{19}F NMR analysis was carried out after standing for 72 h. Integration of the $\delta -75.2$ [s, 3F] peak for the fluoroester relative to the $\delta -62.9$ [s, 3F] peak of TFT allowed quantification of the acid end-groups.

2.11. Preparation of TA and MHET mixture

BHET (3 g) was dissolved in EG (100 ml) and water (20 ml), and then NaOH solution (10 wt%, 3 g) was added [52]. The mixture was heated to 70 °C for 0.5 h, cooled to room temperature, and further NaOH solution (5 g) was added. After 2 h, sulfuric acid was added when a mixture of TA and MHET precipitated. The precipitate was thrice washed with water and filtered, and finally dried. ^1H NMR in $CDCl_3$–HFIP mixture (95:5, by weight): MHET: $\delta = 8.137$ (s, 4H), 4.032 (t, 2H) 4.516 (t, 2H). ^1H NMR in DMSO: TA: δ 8.05 (s, 4H) ppm, MHET: δ 8.096 (d, $J = 4.0$, 4H), 3.735(t, 2H), 4.327(t, 2H).

2.12. Fluoroesterification of acid mixture or sublimate

0.002 g of the TA and MHET mixture (Section 2.11), or of the sublimate (Section 2.8), was added to 1 g of $CDCl_3$–HFIP mixture (95:5, by weight). 4-pyrrolidinopyridine (0.0001 g) and DCC (0.001 g) were each added as solution in $CDCl_3$ (0.1 g). ^1H NMR peaks at δ 8.256 (s, 4H), 6.01(septet, 2H) correspond to the diester of TA,

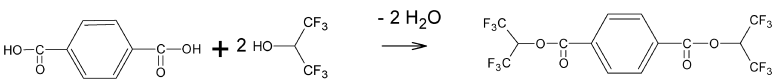

(12)

and the peaks δ 8.19 (d, 4H, $J = 2.8$), 6.01(septet, 1H), 4.02 (t, 2H), 4.52 (t, 2H) correspond to the fluoroester of MHET:

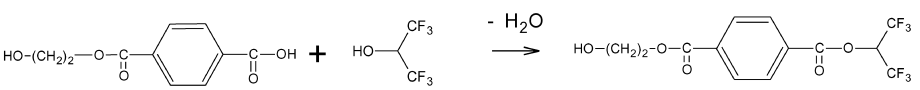

(13)

3. Results and discussion

The IV vs. time data for SSP of the 180 μm thick disks at 250 °C are shown in Fig. 1. Initially, the IV increases quickly during SSP-vacuum, and then nearly flattens out at a maximum IV of 2.75 dl/g at 6 h. This kinetic data represents much faster SSP as compared with the previously reported experiments. For example, Hsu [8], Rinehart [39], Ito et al. [40] and Boiko and Marikhin [24] reported the time required for reaching IV ~ 2.4 (or $M_n = 130,000$) as 35, 5, 7, and 10 h, respectively, as

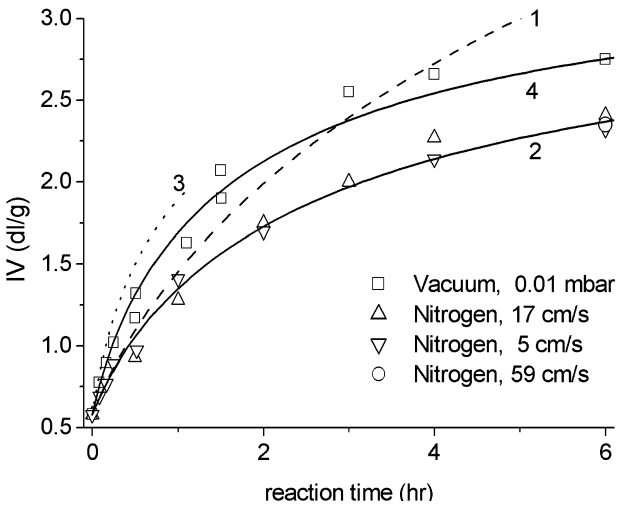

Fig. 1. Increase in IV with time of SSP reaction in 180 μm thick PET chips at 250 °C in vacuum (10 mtorr) or under nitrogen flow (at the indicated gas velocities). Curve 1: fit to SSP-N_2 (5 cm/s) data up to 1 h while considering all end-groups to be active (Eqs. (3)–(7)). Curve 2: fit to all SSP-N_2 (5 cm/s) data while accounting for a part of the acid and hydroxyl end-groups to be inactive (Eqs. (15) and (16)). Curve 3: prediction for SSP-vacuum assuming kinetics control (Eqs. (26)–(28)) for removal of aromatic condensates. Curve 4: fit to SSP-vacuum data assuming mass transfer control (Eqs. (29)–(31)) for removal of aromatic condensates.

compared to 3 h in our SSP-vacuum experiments. Further, we notice from Fig. 1 that the SSP proceeds faster in vacuum as compared to SSP under nitrogen sweep. This is also indicated by the faster depletion of the end-groups during SSP-vacuum as compared to SSP-N_2 (Fig. 2).

The results of Figs. 1 and 2 are replotted in Fig. 3 to show the dependence of the end-group concentrations on IV. The overlap of this dependence for SSP-N_2 and SSP-vacuum (Fig. 3) indicates that even though the overall rate of reaction is enhanced by vacuum (Figs. 1 and 2), the end-group pattern remains similar for SSP-N_2 and SSP-vacuum when a comparison is made at the same molecular weight. Fig. 4 shows the relation between the measured IV (Fig. 1) and the M_n calculated (Eq. (5)) from the measured end-group concentrations. A least-square straight-line fit on the logarithmic plot yields the following Mark-Houwink relation in phenol-TCE (1:1 by wt) at 30 °C:

$$\mathrm{IV} = 1.175 \times 10^{-3} M_n^{0.627} \quad \text{for } 0.58 < \mathrm{IV} < 2.75 \tag{14}$$

which is shown as a dotted line in Fig. 4. For comparison, also shown (as continuous lines) are the previously reported Mark-Houwink relations (Eq. (9), Table 3). The differences between the previously reported measurements and our results could be related to the following: different temperatures for viscosity measurement, limited accuracy of the IV and end-group concentration measurements, different extent of additional (such as vinyl) end-groups present in the PET used, a smaller range of M_n (<30,000) examined by the previous workers, limited accuracy of the IV-η_{rel} approximation (Eq. (8)), etc.

3.1. SSP-N_2 kinetics and crystallization induced chain-end immobility

We notice from Fig. 1 that the kinetics of SSP-N_2 is not affected by increasing the nitrogen flow velocity beyond 5 cm/s, indicating that gas phase mass transfer is not the rate controlling step under these conditions. In case of thick PET (half thickness, $L > \sqrt{D/(kC)}$, where D and C are the condensate diffusivity and concentration, and k is the corresponding rate constant [11]), the SSP can be limited by the outward diffusion of the condensates EG and water through the polymer. Calculation with $D_{EG} = 3.1 \times 10^{-6}$ cm^2/s [21], $k = 0.0115$ kg/mequiv. h (this paper), and $C =$ 82 mequiv./kg (this paper) suggests that such diffusional limitations are negligible at chip thickness of 180 μm

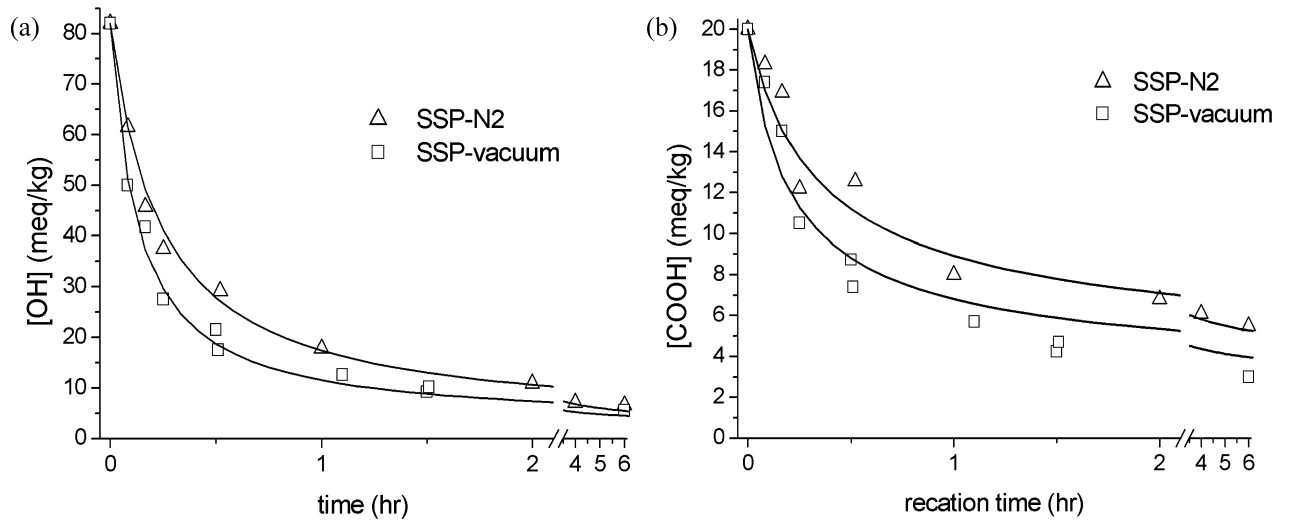

Fig. 2. Depletion of the (a) hydroxyl and (b) acid end-groups with time of SSP reaction in 180 μm thick PET chips at 250 °C in vacuum (10 mtorr) or under nitrogen flow (5 cm/s). The upper lines represent the fits to SSP-N_2 (5 cm/s) data while accounting for the inactive end-groups, and the lower lines represent the fit to SSP-vacuum data assuming mass transfer controlled removal of aromatic condensates.

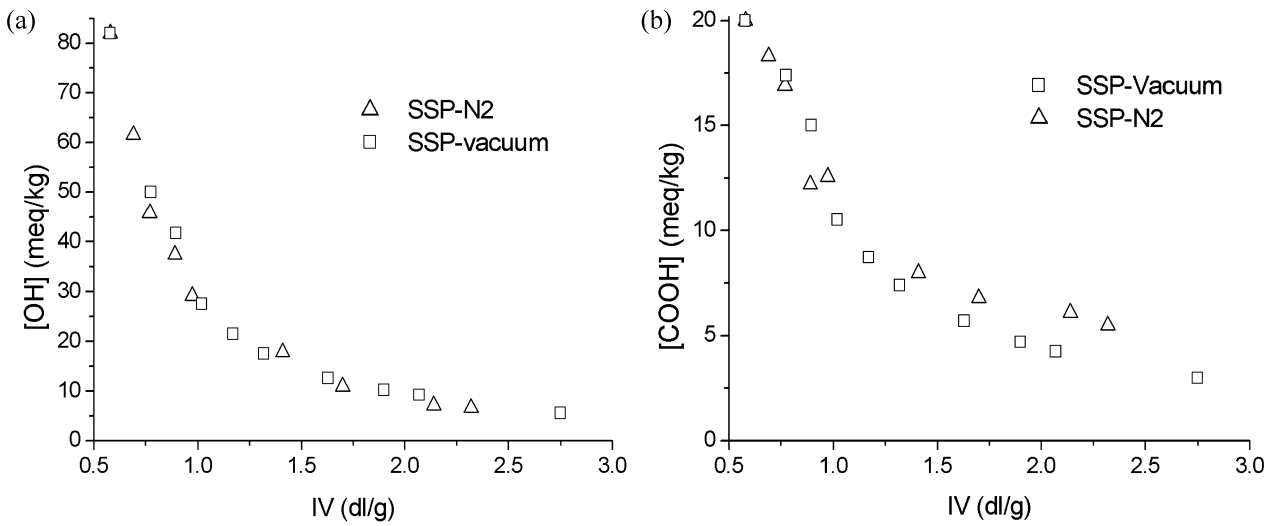

Fig. 3. Depletion of the (a) hydroxyl and (b) acid end-groups with increase in IV during SSP reaction in 180 μm thick PET chips at 250 °C in vacuum (10 mtorr) or under nitrogen flow (5 cm/s).

employed in this work. Hence, the observed rate of our SSP reaction must be limited by the intrinsic reaction kinetics, and we will like to represent our SSP kinetics data in terms of the reactions (1) and (2). We are reminded that several possible side reactions can result in additional consumption/production of the hydroxyl and acid end-groups, and lead to formation of vinyl and diethylene glycol end-groups, acetaldehydes, and crosslinks [2,13]. However, considering the moderate temperature (as compared to melt polymerization) and inert atmosphere (e.g. oxygen is known to accelerate degradation rate [2]) involved in our work, we keep our kinetics analysis simple by ignoring these side reactions and additional end-groups, and their influence on M_n (Eq. (5)) and hence on the Mark-Houwink relationship (Eq. (9)).

First, the kinetics data ([OH](t) and [COOH](t)) in the initial stage (IV up to 1.5 dl/g) of SSP-N_2 (5 cm/s) are fitted with the kinetics expressions Eqs. (3)–(7) (using the CONSTANT_RELATIVE_VARIANCE model of the gPROMS software, PSE Enterprises, UK) to estimate the rate constants: $k_1 = 0.0111$ kg/mequiv. h and $k_2 = 0.0264$ kg/mequiv. h. These values can be compared with Kang's analysis [21] of the experiments of Chen and Chen [3] resulting in $k_1 = 0.009$ kg/mequiv. h and $k_2 = 0.0143$ kg/mequiv. h at 230 °C, though most likely with a different catalyst composition. The fitted curve 1 (Fig. 1) deviates from our experimental values at the larger time ($t > 1$ h). This is because the reaction rate at this time is strongly influenced by inability of a part of end-groups to participate in the condensation reactions (Eqs. (1) and (2)). Zhi-Lian et al. [14], Wu et al. [23] and Kang [21] did not notice such inconsistency because their experimental observations were limited to M_n less than 52,000. Duh [16] accounted for such inactive groups, but its enormous impact was not visible in their analysis limited to IV less than 1.3 dl/g. Our fitted results (curve 1 of Fig. 1) indicates that the SSP-N_2 data at such IV (< 1.3 dl/g) can easily be represented even while neglecting the effect of such inactive groups. Though the concentration of such groups is small, they make up an increasing fraction of the total number of end-groups with progress of SSP. The inability of a part of the end-groups to participate in the polycondensation reactions can be either due to chemical degradation leading to unreactive chain ends (such as vinyl end-groups), or due to the reactive ends being unable to approach each other. Such limited extent of mobility of some chain-ends could be a result of their being restricted by relatively short chain segments linking them to crystalline parts, or a result of their having been incorporated in crystalline parts as defects. We note from Fig. 2 that the OH and the COOH end-groups are still detectable (by fluoroderivatization and ^{19}F NMR), at substantial concentrations of 5 mequiv./kg and 3 mequiv./kg, respectively, at

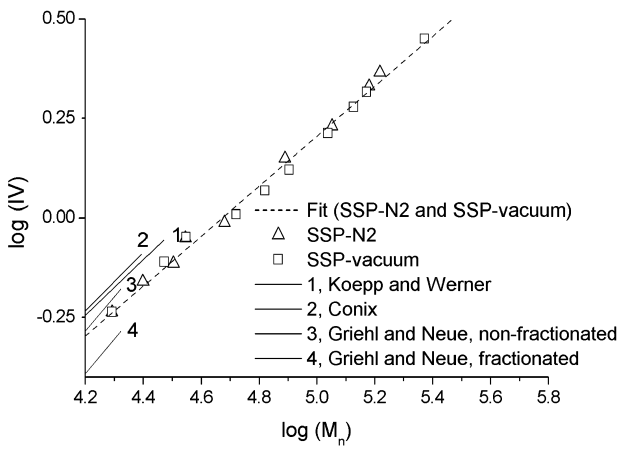

Fig. 4. Mark-Houwink relationship between the measured IV (Section 2.3) and M_n (determined from the end-group measurements of Section 2.9 and 2.10) of the PET samples obtained during SSP-N_2 and SSP-vacuum. The dotted line is the least square fit on the logarithmic plot, resulting in Eq. (14). The continuous lines correspond to previously reported relations (Eq. (9), Table 3).

the end of our SSP-vacuum where the observed reaction rate is very low compared to the SSP rate expected if some of these were not temporarily inactivated (Fig. 1). We verified this by the following experiment: starting with the PET sample of IV = 2.75 dl/g (obtained by SSP-vacuum, $t = 6$ h as in Fig. 1), a continued SSP-vacuum at 250 °C for further 4 h resulted in no further increase in IV. Four of these PET chips were placed on aluminium foils, and heated under vacuum to melt at 270 °C. After allowing further polymerization in melt for 1.5 h, the chips were examined for IV. The measured IV = 2.97 dl/g represents a re-initiation of the polymerization in melt. We conclude that melting at the apparent end of reaction during SSP results in release of the crystalline restraints on the mobility of the temporarily inactivated acid and hydroxyl end-groups, allowing post polymerization to start again.

This suggests that a kinetic analysis of SSP should take into account this apparent inactivity of a fraction of the OH and COOH end-groups. We consider both the transesterification and the esterification reactions as we monitor both the OH and the COOH end-groups during the SSP:

$$R_{EG} = 2k_1([OH] - [OH]_i)^2 \quad (15)$$

$$R_{H_2O} = k_2([COOH] - [COOH]_i)([OH] - [OH]_i) \quad (16)$$

where $[OH]_i$ and $[COOH]_i$ are the (unknown) concentrations of the temporarily inactivated OH and COOH end-groups during SSP. The IV(t), [OH](t) and [COOH](t) data in the entire range of SSP-N_2 (5 cm/s) are now fitted using the gPROMS software with the kinetics expressions Eqs. (3)–(5),(15) and (16) to estimate the rate constants: $k_1 = 0.0115$ kg/mequiv. h, $k_2 = 0.034$ kg/mequiv. h and the inactive end-group concentrations $[OH]_i = 3.1$ mequiv./kg and $[COOH]_i = 2.8$ mequiv./kg. The corresponding calculated [OH](t), [COOH](t) and IV(t) profiles are shown as curve 2 in Fig. 1, and as upper lines in Fig. 2(a) and (b), and we conclude a satisfactory match with the experimental measurements till IV = 2.3 dl/g obtained by us during SSP-N_2.

We may compare our estimated inactive end-group concentrations (C_i) with the following relation of Duh [16]:

$$C_i = 43.31 + 1.0723C_o - 4.683 \times 10^{-2}T - 2.0755 \times 10^{-3}C_oT \quad \text{for } 200\,°C \le T \le 230\,°C \quad (17)$$

where $C_o = [OH]_o + [COOH]_o = 102$ mequiv./kg is the initial concentration of the reactive groups in PET pellets. When extrapolated to 250 °C, Eq. (17) yields an inactive end-group concentration of 17.5 mequiv./kg. This is far in excess of the $[OH]_i + [COOH]_i = 5.9$ mequiv./kg obtained by us, and indicates that this relation (Eq. (17)) cannot be extrapolated to the SSP conditions employed by us.

3.2. SSP-vacuum

Fig. 1 indicates that under otherwise identical conditions, SSP proceeds significantly faster in vacuum as compared to the SSP under N_2 sweep. We do not expect an influence of the inert surrounding media on the intrinsic reactions, but an influence on mass transfer of the condensates by one of the following mechanisms is a possibility:

(1) faster removal of water or EG when vacuum is applied
(2) removal of other end-group containing molecules under vacuum.

As discussed in Section 3.1, removal of water and EG through the polymer and the surrounding medium is not the rate limiting step during our SSP, and hence hastening of these steps during SSP-vacuum cannot explain the observed increase in the overall reaction rate during SSP-vacuum as compared to SSP-N_2. Our following observation of the solid deposits (sublimate) on the cold parts of the reactor walls during SSP-vacuum (Section 2.8) and not during SSP-N_2 (Section 2.6) points to the possibility (2) above, and we carry out an analysis of the constituents of the sublimate. Higher vacuum levels resulting in supersaturation of solutes are known [53,54] to enhance diffusive devolatilization of solutes from polymer matrices.

3.2.1. Characterization of sublimate from SSP-vacuum

^{1}H NMR spectrum of the sublimate (Section 2.8) in $CDCl_3$–HFIP (95:5 by wt) mixture is shown in Fig. 5(a). The singlets at δ 8.08 and 4.69 are attributed [55] to the cyclic oligomers of PET. The singlet at δ 8.115 (4 H) and the triplets at δ 4.035 (4H) and δ 4.505 (4H) are attributed to BHET, and we verified this by addition of additional BHET that resulted in enhancement of these peaks. The singlet at δ 8.137 is attributed to MHET (Section 2.11). This was confirmed by a DCC-mediated esterification of the sublimate with HFIP (Section 2.12), when a doublet at δ 8.19 ($J = 2.4$) featured (Fig. 5(b)) corresponding to the hexafluroisopropyl ester of MHET (Section 2.12). In addition, a singlet at δ 8.256 featured (Fig. 5(b)) corresponding to diester of TA (Section 2.12), indicating that TA was constituent of the sublime, but was not detected in the ^{1}H NMR of the sublime (Fig. 5(a)) because it is insoluble in the $CDCl_3$–HFIP mixture. The composition of the sublimate so determined, is shown in Table 4. During LC–MS (Section 2.4) of the SSP-vacuum sublimate, the species eluted at 2.88 and 3.13 min were detected to have molecular weights of 243 and 277, respectively, corresponding to ionized MHET and BHET, thus further verifying the presence of MHET and BHET in the sublimate.

3.2.2. Reactions responsible for the aromatic condensates in sublimate

The extraction of cyclic oligomers at high vacuum during melt polymerization reactions is well known [27]. These

cyclic oligomers (primarily trimers) are believed to be formed mainly by transesterification of hydroxyl chain-ends [56,57]. Added presence of TA, MHET and BHET in the sublimate during SSP-vacuum indicates that these are formed as condensates during SSP by the following reactions, and their removal from the PET chips by high vacuum enhances the rate of rise of IV during SSP-vacuum as compared to SSP-N_2:

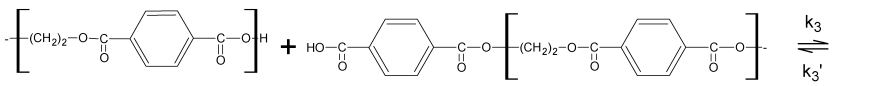

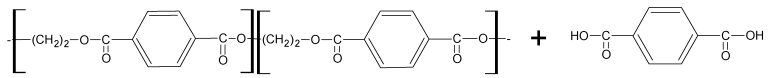

(18)

(TA)

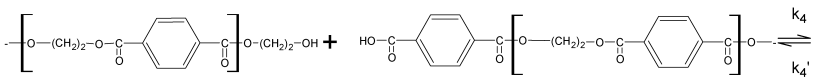

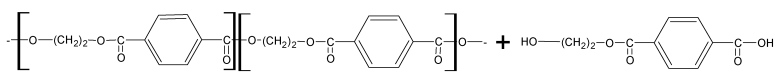

(19)

(MHET)

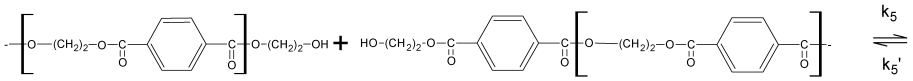

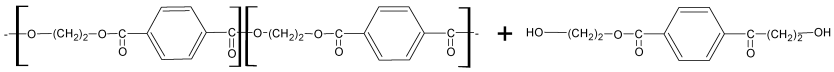

(20)

(BHET)

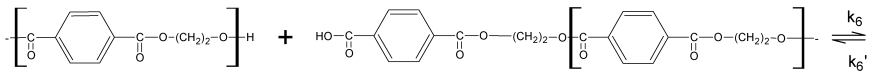

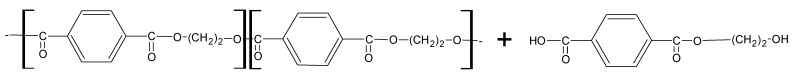

(21)

(MHET)

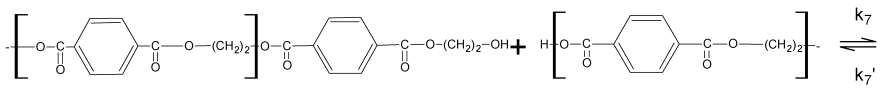

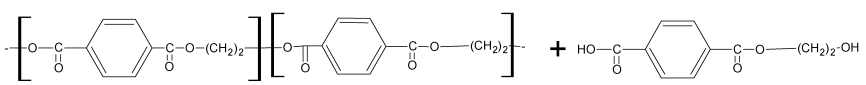

(22)

(MHET)

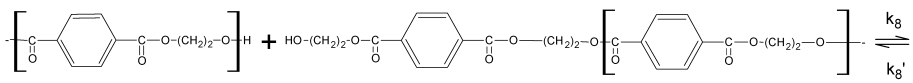

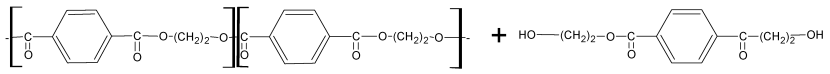

(23)

(BHET)

Though these are essentially the well known intermolecular glycolysis, acidolysis and transesterification reactions [58,59], their importance in the overall progress of polymerization has not been realized in the past. If an instantaneous removal of TA, MHET and BHET during SSP was possible, incorporation of these reactions in the kinetic scheme along with

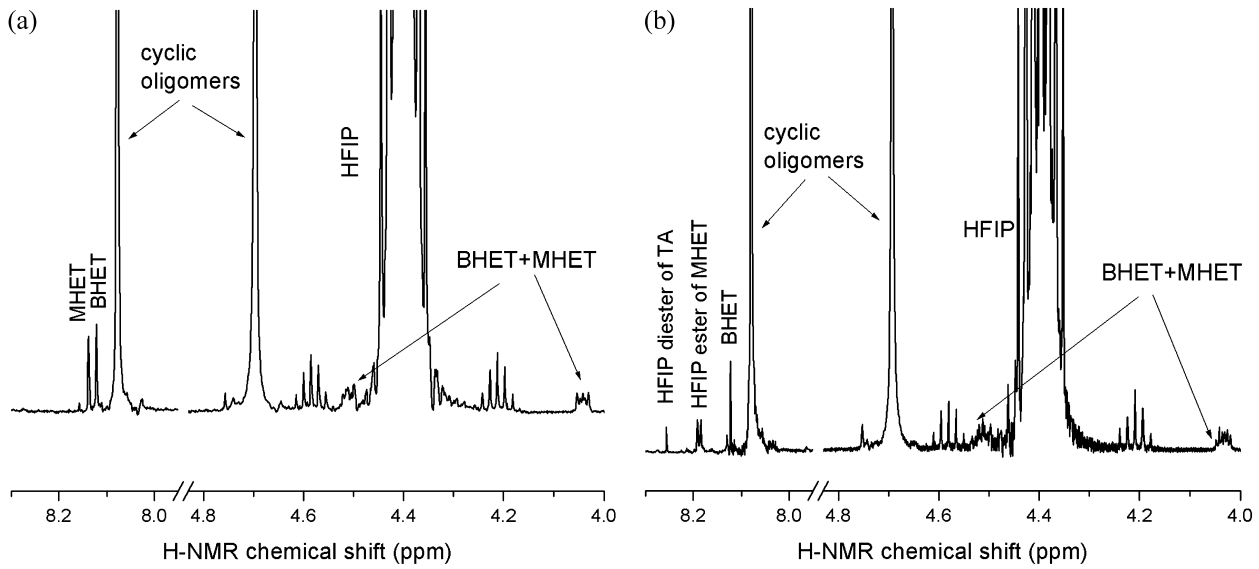

Fig. 5. ^{1}H NMR of the sublimate obtained during SSP-vacuum, (a) as obtained in Section 2.7, and (b) after esterification with HFIP (Section 2.12).

transesterification and esterification reactions (Eqs. (1) and (2)) would lead to the following modification of the reaction kinetics (Eqs. (3) and (4)):

$$\frac{d[OH]}{dt} = -2R_{EG} - R_{H_2O} - 2R_{BHET} - R_{MHET} \quad (24)$$

$$\frac{d[COOH]}{dt} = -R_{H_2O} - R_{MHET} - 2R_{TA} \quad (25)$$

where the EG and water production rates would continue to be described by Eqs. (15) and (16), and we can estimate the maximum rates of production (and removal) of TA, MHET and BHET in the absence of the reverse reaction as:

$$R_{TA} = 2k_3([COOH] - [COOH]_i)^2 \quad (26)$$

$$R_{MHET} = (k_4 + k_6 + k_7)([COOH] - [COOH]_i)([OH] - [OH]_i) \quad (27)$$

and

$$R_{BHET} = 2(k_5 + k_8)([OH] - [OH]_i)^2 \quad (28)$$

where we have again assumed the reaction rates to be dependent only on the reactive chain-ends. We further approximate $k_3 = k_4 = k_5 = k_6 = k_7 = k_8 \approx k_1$, as Kotliar [59] estimated the polycondensation and redistribution rates to be comparable (at 254 °C). Solving the initial value problem posed as Eqs. (24)–(28) as well as Eqs. (15) and (16) using the $k_1, k_2, [OH]_i, [COOH]_i$ values as obtained from SSP-N_2 experiments, we find the predicted IV(t) profile (curve 3 in Fig. 1) at short time (<1 h) to be much faster than the SSP-vacuum observations of Fig. 1. Thus, as expected, the rate of removal of the aromatic condensates TA, MHET and BHET must be far short of their maximum possible production rate estimated from kinetics of the forward reaction alone (Eqs. (26)–(28)). Hence, the net contribution of the reactions (Eqs. (18)–(23)) to the progress of SSP-vacuum can be expected to be controlled by the rate of mass transfer of the aromatic condensates.

Table 4
Composition of the SSP-vacuum (250 °C, 3 h) sublimate (Section 2.8) as determined by ^{1}H NMR (Fig. 5)

Constituents	Mole fraction (aromatic rings)
Cyclic oligomers (trimers)	0.92
BHET	0.035
MHET	0.037
TA	0.007

3.2.3. Mass transfer controlled removal of aromatic condensates during SSP-vacuum

A realistic analysis should consider simultaneously the reaction kinetics, and mass-transfer (both through the polymer and the surrounding medium, as influenced by the reduced pressure [53,54]) of the aromatic condensates. However, this is formidable in the absence of data such as all kinetic rate constants (Eqs. (18)–(23)) and diffusivities and mass-transfer coefficients, and we simply lump these effects [60] by writing the rates of removal of TA, MHET and BHET in terms of the corresponding (unknown) overall mass transfer coefficients k_{TA}, k_{MHET} and k_{BHET} :

$$R_{TA} = k_{TA}[TA] \quad (29)$$

$$R_{MHET} = k_{MHET}[MHET] \quad (30)$$

and

$$R_{BHET} = k_{BHET}[BHET] \quad (31)$$

We shall further consider the concentrations of TA, MHET and BHET in the PET chips during SSP-vacuum to be determined by (pseudo) equilibrium considerations. Using equal reactivity hypothesis and probabilistic arguments [61]

we can arrive at the following:

$$\frac{[TA]}{[P]} = \frac{[COOH]}{[COOH]+[OH]}(1-p_{COOH}) \quad (32)$$

$$\frac{[MHET]}{[P]} = \frac{[COOH]}{[COOH]+[OH]}p_{COOH}(1-p_{OH}) \quad (33)$$

$$\frac{[BHET]}{[P]} = \frac{[OH]}{[COOH]+[OH]}p_{OH}p_{COOH}(1-p_{OH}) \quad (34)$$

where

$$[P] = \frac{[COOH]+[OH]}{2}$$

refers to molar concentration of all (macro)molecular species in the PET undergoing SSP,

$$p_{COOH} = \frac{[COO]}{[COO]+[COOH]}$$

and

$$p_{OH} = \frac{[COO]}{[COO]+[OH]}$$

refer to the fraction of reacted COOH and OH groups in the PET, and [COO] refers to the concentration of the ester groups. Under the simplification [COOH] $\ll$ [COO] and [OH] $\ll$ [COO], this leads us to:

$$[TA] = \frac{[COOH]^2}{2[COO]} \quad (35)$$

$$[MHET] = \frac{[COOH][OH]}{2[COO]} \quad (36)$$

$$[BHET] = \frac{[OH]^2}{2[COO]} \quad (37)$$

Further, considering the presence of inactive end-groups, [OH] and [COOH] in the Eqs. (32)–(37) should be replaced by ([OH] − $[OH]_i$) and ([COOH] − $[COOH]_i$), respectively. We will now like to determine the yet unknown mass transfer coefficients by fitting the SSP-vacuum data in the form of IV(t), [OH](t) and [COOH](t) (Fig. 2(a) and (b)) with the rate expressions Eqs. (15),(16),(24),(25),(29)–(31) and (35)–(37). With the limited experimental data available here, it seems unreasonable to try to estimate the three different mass transfer coefficients. In the absence of a more suitable interrelation, we make a somewhat gross approximation $k_{TA} = k_{MHET} = k_{BHET} = k$(say), and then use gPROMS to fit the SSP-vacuum data (Figs. 1 and 2), thereby estimating the overall mass transfer coefficient k = 405 /h, or the corresponding surface area based mass transfer coefficient $k' = kL = 0.06$ cm/min. The corresponding calculated IV(t), [OH](t) and [COOH](t) profiles for SSP-vacuum are shown as curve 4 in Fig. 1, and as lower lines in Fig. 2(a) and (b). We conclude a satisfactory match with the experimental measurements till IV = 2.75 dl/g obtained by us, suggesting that the enhancement in overall reaction rate during SSP-vacuum as compared to SSP-N_2 can be attributed to the mass transfer controlled removal of the end-group containing aromatic condensates during SSP-vacuum. While our experimental measurements indicate leveling out of the IV increase during SSP at 6 h, the predicted curves still show an increasing trend. This may be because the so termed inactive end-groups are not all inherently inactive to begin with, but some are rendered inactive during the SSP by the progressing crystallization. Though a theoretical modeling of such an effect is not presently possible, its consideration would have predicted a sharper slowdown in the SSP reaction, perhaps in better agreement with our experimental observation.

4. Conclusions

We have analyzed the kinetics of SSP of thin PET chips at 250 °C in two different reaction environments: fast flowing nitrogen and high vacuum. The post polymerization begins with efficient removal of EG and water as condensates, but slows down considerably at IV > 1.3 dl/g due to the restricted mobility of a part of the chain-ends due to crystalline restraints. This is verified by detection of substantial concentration of the hydroxyl and acid end-groups at IV = 2.75 dl/g at the end of SSP-vacuum, and further post-polymerization only after melting to impart mobility to these end-groups. An analysis of the sublimate during SSP-vacuum shows that TA, MHET and BHET are removed from the PET chips at the high temperature and vacuum applied. These functional end-group carrying aromatic molecules are considered to be produced by acidolysis, glycolysis and transesterification reactions. Their removal as a sublimate during SSP under vacuum provides an additional pathway for the progress of SSP, albeit limited by mass transfer even in the thin PET chips considered here.

References

[1] Schaaf E, Zimmerman H, Dietzel W, Lohmann P. Acta Polymerica 1981;32:250.
[2] Ravindranath K, Mashelkar RA. Chem Engng Sci 1986;41:2197.
[3] Chen S-A, Chen F-L. J Polym Sci, Part A: Polym Chem 1987;25:533.
[4] Duh B. J Appl Polym Sci 2002;83:1288.
[5] Marechal E. In: Fakirov S, editor. Polyesters: synthesis and chemical aspects. Handbook of thermoplastic polyesters, vol. 1. New York: Wiley; 2002. p. 1.
[6] Aharoni SM. In: Fakirov S, editor. Industrial scale production of polyesters. Handbook of thermoplastic polyesters, vol. 1. New York: Wiley; 2002. p. 56.
[7] Wendling PR. US Patent 4532319; 1985.
[8] Hsu L-C. J Macromol Sci—Phys 1967;B1(4):801.
[9] Chen FC, Griskey RG, Beyer GH. AIChEJ 1969;15:680.
[10] Jabarin SA, Lofgren EA. J Appl Polym Sci 1986;32:5315.
[11] Ravindranath K, Mashelkar RA. J Appl Polym Sci 1990;39:1325.
[12] Fakirov S. In: Schultz JM, Fakirov S, editors. Solid state reactions in linear polycondensates. Solid state behavior of linear polyesters and polyamides, Prentice Hall: New Jersey; 1990. p. 1.

[13] Devotta I, Mashelkar RA. Chem Engng Sci 1993;48:1859.
[14] Zhi-Lian T, Gao Q, Nan-Xun H, Sironi C. J Appl Polym Sci 1995;57:473.
[15] Huang B, Walsh JJ. Polymer 1998;39:699.
[16] Duh B. J Appl Polym Sci 2001;81:1748.
[17] Gaymans RJ, Amrithraj J, Kamp H. J Appl Polym Sci 1982;27:2513.
[18] Kaushik A, Gupta SK. J Appl Polym Sci 1992;54:507.
[19] Warner SB, Lee J. J Polym Sci, Polym Phys Ed 1994;32:1759.
[20] Srinivasan R, Almonacil C, Narayan S, Desai P, Abhiraman AS. Macrmolecules 1998;31:6813.
[21] Kang C-K. J Appl Polym Sci 1998;68:837.
[22] Mallon FK, Ray WH. J Appl Polym Sci 1998;69:1233.
[23] Wu D, Chen F, Li R, Shi Y. Macromolecules 1997;30:6737.
[24] Boiko YM, Marikhin VA. Polym Sci USSR, Ser. A 2000;42:1169.
[25] Medellin-Rodriguez FJ, Lopez-Guillen R, Waldo-Mendoza MA. J Appl Polym Sci 2000;75:78.
[26] Gao Q, Nan-Xun H, Zhi-Lian T, Gerking L. Chem Engng Sci 1997;52:371.
[27] Chang TM. Polym Engng Sci 1970;10:364.
[28] Chang S, Sheu M-F, Chen SM. J Appl Polym Sci 1983;28:3289.
[29] Karayannidis GP, Kokkalas DE, Bikiaris DN. J Appl Polym Sci 1995;56:405.
[30] Kokkalas DE, Bikiaris DN, Karayannidis GP. J Appl Polym Sci 1995;55:787.
[31] Duh B. Polymer 2002;43:3147.
[32] Gupta SK, Kumar A. Reaction engineering of step growth polymerization. New York: Plenum Press; 1987. p. 285.
[33] Ito M, Takahashi K, Kanamoto T. J Appl Polym Sci 1990;40:1257.
[34] Ziabicki A. Text Res J 1996;66:705.
[35] Huang B, Tucker PA, Cuculo JA. Polymer 1997;38:1101.
[36] Kurita K, Hayashi M, Ohta T, Ishihara H, Okada F, Yoshikawa W, Chiba A, Tate S. US Patent 4851508; 1989.
[37] Cohn G. Polym Prepr 1989;30:160.
[38] Cohn G. US Patent 4792573; 1988.
[39] Rinehart VR. US Patent 4755587; 1988.
[40] Ito M, Wakayama Y, Kanamoto T. Polymer 1992;48:569.
[41] Ito M, Wakayama Y, Kanamoto T. Sen-I-Gakkaishi 1994;35:1210.
[42] Sasaki I, Mori H, Fujimoto M. EP0182352; 1985.
[43] Jabarin SA. Polym Mater Encyclopedia 1996;8:6078.
[44] Schaaf E, Zimmermann H. East Ger Patent, 139,129; 1979.
[45] Mallon F, Beers K, Ives A, Ray WH. J Appl Poym Sci 1998;69:1789.
[46] Ma Y, Agarwal US, Vekemans JAJM, Sikkema DJ. Polymer 2003; in press.
[47] Solomon OF, Ciuta IZ. J Appl Polym Sci 1962;6:683.
[48] Koepp HM, Werner H. Makromol Chem 1959;32:79.
[49] Conix A. Makromol Chem 1958;26:226.
[50] Griehl W, Neue S. Faserforsch Textiletechn 1954;5:423.
[51] Kenwright AM, Peace SK, Richards RW, Bunn A, MacDonald WA. Polymer 1998;40:2035.
[52] Hotten BW. Ind Engng Chem 1957;49:1691.
[53] Biesenberger JA, Sebastian DH. Polymer devolatilization. Principles of polymerization engineering, Wiley: New York; 1983. p. 573.
[54] Ravindranath K, Mashelkar RA. Chem Engng Sci 1988;43:429.
[55] Byrant JJL, Semlyen JA. Polymer 1997;38:2475.
[56] Peebles LH, Huffman MW, Ablett CT. J Polym Sci (A-1) 1969;7:479.
[57] Ha WS, Choun YK. J Polym Sci, Polym Chem 1979;17:2103.
[58] Ravindranath K, Mashelkar RA. Chem Engng Sci 1986;41:2969.
[59] Kotliar AM. J Polym Sci, Macromol Rev 1981;16:367.
[60] Maffettone PL, Astarita G, Cori L, Carnelli L, Balestri F. AICHE J 1991;37:724.
[61] Peebles LH. Molecular weight distributions in polymers, 1st ed. New York: Interscience; 1971.